Analyst

Exploration of interactions between membrane proteins embedded in supported lipid bilayers and their antibodies by reflectometric interference spectroscopybased sensing

Journal:	*Analyst*
Manuscript ID:	AN-ART-05-2014-000925.R1
Article Type:	Paper
Date Submitted by the Author:	12-Aug-2014
Complete List of Authors:	Kurihara, Yoshikazu; KONICA MINOLTA, Inc., Sawazumi, Tsuneo; KONICA MINOLTA, Inc., Takeuchi, Toshifumi; Kobe University, Graduate School of Engineering

Journal Name

RSCPublishing

ARTICLE

Exploration of interactions between membrane proteins embedded in supported lipid bilayers and their antibodies by reflectometric interference spectroscopy-based sensing

Cite this: DOI: 10.1039/x0xx00000x

Received 00th January 2012,
Accepted 00th January 2012

DOI: 10.1039/x0xx00000x

www.rsc.org/

Yoshikazu Kurihara,[a,b] Tsuneo Sawazumi,[b] and Toshifumi Takeuchi[a*]

A microfluidic reflectometric interference spectroscopy (RIfS)-based sensor was fabricated to investigate the activity of multidrug resistance-associated protein 1 (MRP1), applied as a model membrane protein. Vesicles containing MRP1 were immobilized simply by injecting a vesicle solution (50 μg/mL) onto a zirconium oxide (ZrO_2) chip under constant flow conditions. Monitoring the shift of the minimum reflectance wavelength (Δλ) of the RIfS demonstrated that the vesicles were adsorbed onto the ZrO_2 chip in a Langmuir-like fashion and suggested that the lipid bilayer structure was preserved on the ZrO_2 chip. The theoretical maximum physical thickness of the layer was 4.97 nm, which was close to the values previously reported for supported lipid bilayers (4.2 to 5.2 nm). When a model protein, the anti-MRP1 antibody (1-50 μg/mL), was injected onto the MRP1-immobilizing ZrO_2 chip a concentration-dependent increase in Δλ was observed. In contrast, a ZrO_2 chip on which the supported lipid bilayers did not contain MRP1 exhibited no response. Moreover, an anti-human IgG antibody generated no change in Δλ, confirming that anti-MRP1 antibodies were selectively bound to the MRP1 immobilized on the chip. These results show that the RIfS sensor can follow specific binding events of biologically active membrane proteins and represents a simple, label-free system capable of facilitating biomedical investigations.

Introduction

Significant research into modeling system architectures with the aim of evaluating the activity of membrane proteins has taken place over the past few decades, since membrane proteins play key roles in various biological systems such as ion channels[1] and serve as carriers or transporters of substances including sugars,[2] amino acids[3] and nucleotides,[4] as well as acting as pumps for active transport,[5] enzymes[5] and receptors.[6] Supported lipid bilayer (SLB) systems have proven to be very useful as a means of understanding signal transduction mechanisms in important biological processes such as these. McConnell et al., considered pioneers of the use of SLBs, established a technique for the immobilization of phospholipid vesicles containing transmembrane proteins, known as vesicle fusion,[7,8] and demonstrated that vesicles spontaneously fuse to form planar membranes when incubated on treated glass surfaces. Subsequently, various other surfaces have been studied, including SiO_2,[9] mica,[10] silicon,[11] gold[12] and glass.

SLBs exhibit higher stability than other artificial model membranes (such as liposome or black lipid membranes) because of their immobilization on a solid support. These layers thus allow the measurement of membrane structures and physical properties using surface analytical methods such as cyclic voltammetry (CV),[13] surface plasmon resonance (SPR),[11] quartz crystal microbalance (QCM)[10] and atomic force microscopy (AFM).[10] Furthermore, SLBs can be formed into patterned or accumulated model membranes using a microfabrication technique.[14,15] Although these characteristics render SLBs suitable for applications in instrumentation devices with the potential for industrial applications, effective methods for studying membrane proteins are still not established, since the above techniques are often complicated and time-consuming. Therefore, there is a demand for simple, rapid and highly selective detection platforms that allow the measurement of the activity of membrane proteins.

We present herein a new method for the investigation of interactions between membrane proteins in SLBs and antibodies, using a reflectometric interference spectroscopy (RIfS)-based sensor. The principle of RIfS is shown in Figure 1. Irradiation of a ZrO_2 sensor chip with incident light (applying vertical incidence in the actual system) produces light reflected from both the ZrO_2 thin film and the silicon substrate material, thus generating interference. The adsorption of ligands on the sensor chip increases the optical film thickness, and thus modifies the reflective interference. Analyzing this

change by spectroscopic means, it becomes possible to ascertain both the adsorption of a substance and the resulting film thickness. RIfS is a technique that potentially allows for simple, label-free detection using white light interference. Sandström et al. noted that the interference colors are most highly saturated when the reflected intensity of a narrow wavelength band is totally extinguished.[16] For a substrate with a real refractive index n_s and normal incidence, this occurs when the film index, n_f, and the medium index, n_0, have the relationship shown in Eq. (1).

$$n_f = \sqrt{n_0 n_s} \qquad (1)$$

Therefore, in the case of a silicon-based RIfS with a high refractive index (n_s = 3.88 at 632.8 nm), it is easier to detect changes in the interference color when n_f is in the vicinity of 2.0. Biosensors using silicon nitride[17-21] (n_f = 1.9 to 2.1) or TiO_2[22,23] (n_f = 2.60 for rutile to 2.72 for anatase at 550 nm) as an interference layer have already been reported, and the ZrO_2 (n_f = 1.95 at 580 nm) used as the chip surface in this study is also expected to function as an interference layer. Moreover, ZrO_2 has a strong affinity for the phosphate groups in phospholipids through coordinate bonding. This occurs because ZrO_2 possesses empty d orbitals and thus acts as a Lewis acid, while the phosphate moiety has a lone pair of electrons and exhibits Lewis base properties.[24]

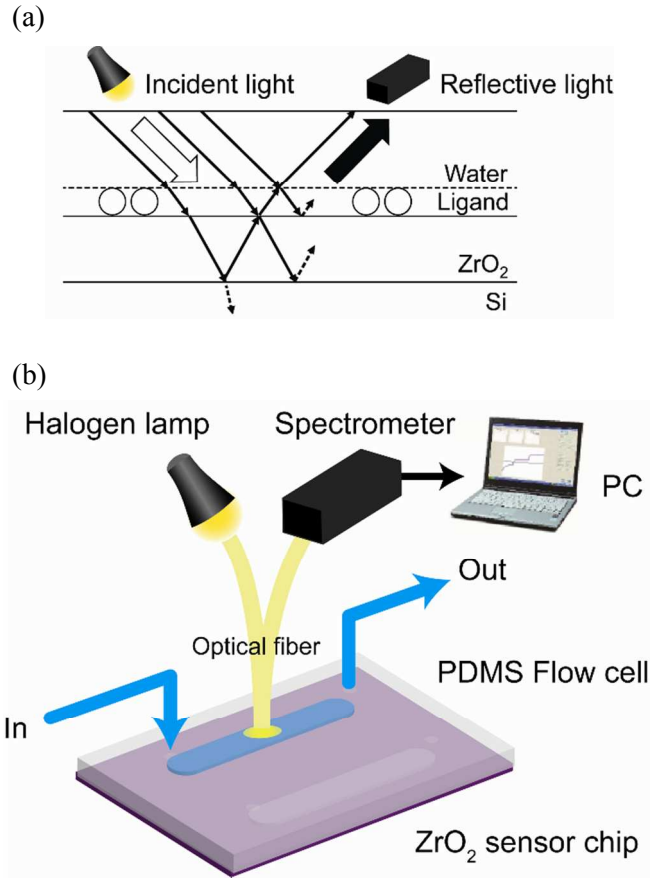

Figure 1. Schematic illustration of (a) the RIfS principle and (b) the RIfS measurement system.

Using this interaction, the selective removal of potassium phosphate by mesoporous ZrO_2 and the selective enrichment of the degradation products of organophosphorus nerve agents such as Sarin by commercially available ZrO_2-coated silica gel beads (HybridSPE™) have been reported.[24,25] There have also been previous reports concerning the use of zirconium phosphate or phosphonate in SLBs.[26-28] Zirconium phosphate or phosphonate immobilized via ionic bond is readily deposited onto a wide range of chips, although it is likely to eventually dissociate from the substrate due to the weak bonding involved.

This paper reports a platform for the real-time detection of membrane protein-protein interactions, primarily based on the application of RIfS together with a continuous-flow microfluidic system consisting of a transparent microfluidic flow cell made of polydimethylsiloxane (PDMS) on a ZrO_2 sensor chip (Figure 1b). A continuous supply of vesicle solution moving through the device ensures that vesicles are gently immobilized on the substrate. As a model membrane protein, we selected multidrug resistance-associated protein 1 (MRP1), which is a 190 kDa transmembrane protein cloned from the drug-selected human small cell lung cancer cells developed by Cole et al. in 1992.[29] This protein was chosen because MRP1 is a very important target in the development of drugs for the treatment of cancer. The core functional unit of MRP1 consists of 17 transmembrane helices and 2 nucleotide binding domains for ATP binding cassettes (ABCs).[30] MRP1 is known to be overexpressed in various human multidrug resistant tumor cell lines and tumors and is capable of excreting natural product drugs, including anthracyclines, *Vinca* alkaloids, taxanes and epipodophyllotoxins by ATP-dependent active transport, leading to multidrug resistance.[31]

Experimental

Reagents and materials

Silicon wafers were purchased from the e-Prize Corp. (Kanagawa, Japan) and ZrO_2 chips fabricated by electron beam evaporation and deposition on silicon wafers were purchased from Seiwa Optical Co., Ltd. (Kanagawa, Japan). Anti-MRP1 antibodies (anti-MRP1, clone: IU2H10 and MRPm5) were obtained from Novus Biologicals, Ltd. (Cambridge, UK). Anti-human IgG antibody (anti-hIgG) was purchased from Acris Antibodies, GmbH (Herford, Germany). Human MRP1 vesicles and control vesicles without MRP1 were acquired from BD Biosciences (5 mg/mL protein; San Jose, CA, USA), which were prepared from insect (Sf9) cells infected with recombinant baculovirus containing human MRP1 gene and wild-type baculovirus, respectively. Dipalmitoylphosphatidylcholine (DPPC) was purchased from the NOF Corp. (Tokyo, Japan). All other reagents were purchased from Wako Pure Chemical Industries, Ltd. (Osaka, Japan).

Immobilization of vesicles on a ZrO_2 chip

In preparation for vesicle loading, a 18 mm × 26 mm × 0.725 mm ZrO_2 chip was exposed to oxygen plasma under air at ca. 5 Pa at a power level in the range of 0.6-1.2 W for 30 s (SEDE-GE; Meiwafosis Co., Ltd., Tokyo, Japan). The plasma-treated ZrO_2 chip and PDMS flow cell (volume: 4 μL, size: 2.5 mm × 16 mm × 0.05 mm) were then affixed to the RIfS apparatus (MI-Affinity LCR-01; Konica Minolta, Inc., Tokyo, Japan) to produce the continuous flow microfluidic RIfS system. The expected incident light intensity was estimated using BK7 chips of the same size as the ZrO_2 chips, purchased from the Shibuya Optical Co., Ltd. (Saitama, Japan). The backs of these chips were painted black to ensure antireflection. The reflected light intensity of the BK7 chips as measured by the RIfS instrumentation was applied as a reference for reflectance simulation calculations using the Essential Macleod software

program (Thin Film Center Inc., Tucson, AZ, USA). Essential Macleod enables the design, analysis, and manufacture of thin film coatings and was employed during this study to calibrate the film reflectance. RIfS data were obtained at a flow rate of 20 µL/min, using a syringe pump (Econoflo Syringe Pump 70-2205, Harvard Apparatus, Holliston, MA, USA) at 25 ºC. A buffer (10 mM Tris-HCl buffer, pH 7.4, 2.7 mM KCl, 140 mM NaCl) was pumped through the apparatus and RIfS measurements were initiated after the baseline had stabilized, indicating that the wavelength corresponding to the minimum value of reflectance (λ) was constant with time. Both MRP1 and control vesicle solutions (protein contents: 5, 10, 50, 100, 250, and 500 µg/mL) were prepared in the same buffer solution and 100 µL aliquots were manually injected at 600 s after the onset of data acquisition. The value of Δλ was determined from the difference between the average value of λ at 600 s ± 15 s and at 1200 s ± 15 s, applying a data acquisition interval of ca. 1 s.

Physical thicknesses of immobilized vesicles

The refractive index (*n*) and extinction coefficient (*k*) of a silicon wafer was measured using a V-VASE ellipsometer (J. A. Woollam Co., Inc., Lincoln, NE, USA). These measurements were performed at incident angles of 70°, 75°, and 80° relative to the surface under ambient conditions and over the spectral range of 300-1200 nm. Ellipsometry data were fitted using the Si.mat model in conjunction with the WVASE32 analysis software package to obtain the optical constants of the silicon wafer. Subsequently, ellipsometry data for ZrO_2 deposited on the silicon wafer were obtained at incident angles of 65°, 70°, and 75° over the spectral range of 400-1000 nm. These data were then fit using the *n* and *k* values of the silicon substrate and applying the Cauchy model (A*n* = 2.00, B*n* = 0.01, C*n* = 0) to obtain the values of *n* and *k* for the ZrO_2 layer and to calculate the layer thickness. The change in Δλ following vesicle adsorption was used to determine the resulting vesicle layer thickness and the associated calculations were performed with the Essential Macleod software program. Reflectance spectra were calculated by employing a multilayer simulation model based on H_2O (medium)/phospholipid/ZrO_2/Si (substrate) and using the optical constants for water provided by Hale[32] together with a reference value of 1.49 for the refractive index of the phospholipid layer.[33,34] As shown in Figure 2, the physical thickness of the adsorbed vesicle layer was estimated using a correlation equation based on a simulation model obtained from the relationship between $\Delta\lambda_{sim}$ and phospholipid layer thickness (Δd_{sim} = 0, 5, 10, 20, 30, 40, or 50 nm). The formula applied to convert $\Delta\lambda_{sim}$ to Δd_{sim} was validated using a Langmuir-Blodgett (LB) monolayer of DPPC prepared in a LB trough (HBM 700 LB, Kyowa Interface Science Co., Ltd., Saitama, Japan). In this process, Milli-Q water containing $CaCl_2$ (3 mM) was used as the subphase, the temperature of which was controlled at 20°C. The surface pressure was measured with a precision of 0.1 mN/m. The lipid concentration was 1 mM and the solution volume spread on the water surface was 100 µL, thus depositing 6×10^{16} molecules at the surface. The DPPC monolayer was spread on the water surface and allowed to stand for at least 1 hour before being compressed to a surface pressure of 30 mN/m, following which the monolayer was transferred to plasma-treated ZrO_2 by pulling a vertical substrate out of the subphase at a deposition rate of 2 mm/min.

Measurement of protein-protein interactions on the immobilized MRP1

A plasma-treated ZrO_2 chip and the PDMS flow cell were attached to the RIfS apparatus to fabricate the continuous flow microfluidic RIfS system. RIfS data were obtained at a flow rate of 20 µL/min using a syringe pump at 25ºC. Measurements were begun after the RIfS baseline had stabilized while running a buffer (10 mM Tris-HCl buffer, pH 7.4, 2.7 mM KCl, 140 mM NaCl), indicating that the wavelength corresponding to the minimum value of reflectance (λ) was constant with time. MRP1 vesicle solution (protein content: 50 µg/mL) or control vesicle solution (protein content: 500 µg/mL) were injected at the 600 s mark. Subsequently, the anti-MRP1 antibody (anti-MRP1, clone: IU2H10 or MRPm5) solution (1, 10, 20, 50, or 100 µg/mL) was injected at 1800 s. The value of Δλ associated with each antigen-antibody iteration was determined from the difference between the average values of λ at 1800 s ± 50 s and at 2400 s ± 50 s.

Results and discussion

In this work, the protein-protein interactions of MRP1 immobilized on a ZrO_2 chip via a SLB were selectively detected, employing the anti-MRP1 antibody (anti-MRP1) as a model protein binder for MRP1. As the first step of MRP1 immobilization via a SLB, the ZrO_2 chips were oxygen plasma-treated to increase their hydrophilicity, which was expected to improve the affinity of the chip surface for the hydrophilic groups of vesicles based on phosphates. Based on the contact angle of the treated chip surfaces with water, super-hydrophilicity was achieved (4.4° ± 0.3°, n=3) and was maintained for 6 hours under atmospheric conditions (see Supporting Information, Figure S1).

Each vesicle adsorption was evaluated by injection of vesicles with or without MRP1 onto the plasma-treated ZrO_2 chips (Figure 2a). As shown in Figure 1a, a concentration-dependent increase in Δλ (the shift of the minimum reflectance wavelength) was observed both with and without the MRP1 (control) vesicles over the range of 1 to 250 µg/mL. These adsorption data were applied to the Langmuir isotherm[35] relationship presented in Eq. (2), where $\Delta\lambda_{max}$ is the maximum shift of Δλ, *C* is the protein concentration in vesicle solution and K_a is the affinity constant associated with vesicle fusion on the plasma-treated ZrO_2 chip.

$$\frac{C}{\Delta\lambda} = \frac{C}{\Delta\lambda_{max}} + \frac{1}{K_a\Delta\lambda_{max}} \qquad (2)$$

The vesicle adsorption data were found to fit the Langmuir isotherm relationship (coefficient of determination $R^2 > 0.92$, Figure 2b). Since the Langmuir equation assumes that adsorption sites are homogeneous and the binding mode is only one to one, this result suggests that the vesicles were simply immobilized on the ZrO_2 chip without forming multilayers. The value of $\Delta\lambda_{max}$ was also calculated from Eq. (2) for each vesicle.

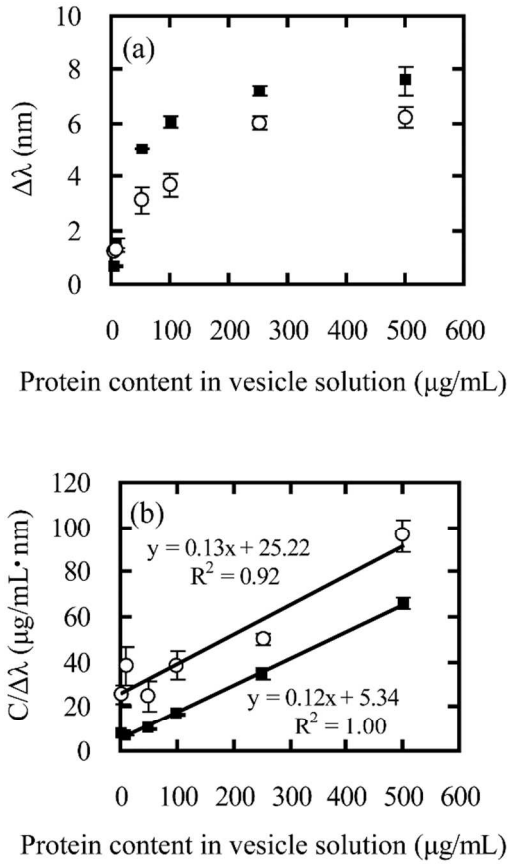

Figure 2. (a) RIfS responses for vesicle adsorption on a ZrO_2 chip and (b) Langmuir isotherms for MRP1 vesicles (solid squares) and control vesicles (open circles). Data points represent the mean ± one standard deviation (SD) of triplicate determinations.

A reflectance simulation model was constructed, based on the optical constants of the silicon wafer and ZrO_2 estimated by ellipsometry (Figure S2) and those of water reported by Hale et al.[32] (Figure 3a). The value of Δλ in this simulation model ($\Delta\lambda_{sim}$) was evaluated for a lipid layer deposited on a ZrO_2 chip and having a refractive index of 1.49[33,34] with a physical thickness (Δd_{sim}) of 0-50 nm (Figure 2b). The results demonstrated that Δd_{sim} was proportional to $\Delta\lambda_{sim}$ and that the ratio of Δd_{sim} to $\Delta\lambda_{sim}$ was 0.60. A dipalmitoylphosphatidylcholine (DPPC) monolayer was deposited onto a ZrO_2 chip by the Langmuir-Blodgett technique to validate this model. The supported DPPC monolayer gave a Δλ value of 4.55 ± 0.16 nm (n=3), which corresponds to a Δd value of 2.73 ± 0.10 nm. This value is comparable to that reported from AFM and mica surface forces measurements (2.5 to 3.0 nm),[36-38] and therefore the RIfS sensor has been shown to be capable of evaluating the physical thickness of the supported lipid layer. The Δd_{max} values obtained from the MRP1 and control vesicles data in Figure 1b were estimated to be 4.99 and 4.52 nm, respectively. These values are in good agreement with the lipid bilayers thicknesses already reported (4.2 to 5.2 nm),[39-42] indicating that both vesicles were immobilized as supported lipid bilayers.

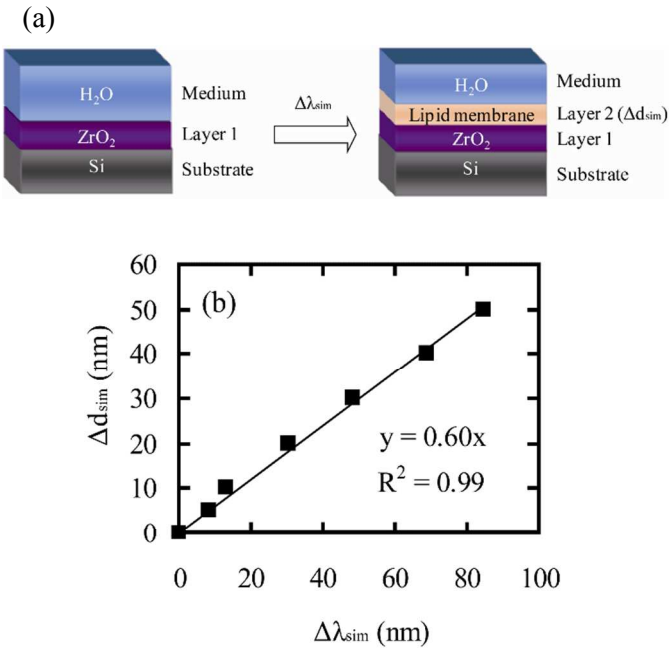

Figure 3. Reflectance simulation model: (a) the layer structures and (b) correlation between $\Delta\lambda_{sim}$ and Δd_{sim}.

The average vesicle sizes determined for the MRP1 and control vesicles from dynamic light scattering (DLS) data were 264 and 667 nm, respectively (Figure S3) and transmission electron microscopy (TEM) revealed that both types of vesicles were of indeterminate form and also confirmed the sizes derived by DLS (Figure S4). When the vesicle size, R, is larger than a critical radius value, R_c (≈ 200 nm), vesicle fusion will occur because the binding energy is higher than the bending energy.[43] These results tend to confirm that the formation of SLBs proceeded on the ZrO_2 chips.

Interactions between the immobilized MRP1 and anti-MRP1 (clone: IU2H10) through the N terminus (amino acids 8-17) of the MRP1 outside of cells *in vivo*[44] (Figure S5) was evaluated by the RIfS sensor. In these trials, Δλ values were measured after injecting an anti-MRP1 solution onto ZrO_2 chips holding either immobilized MRP1 or control vesicles. A concentration-dependent increase in Δλ was observed for the substrate consisting of immobilized MRP1 vesicles (Figure 4a), suggesting that anti-MRP1 interacts with immobilized MRP1 in a quantitative manner. In contrast, the control vesicle-based surface exhibited little change for all concentrations of the anti-MRP1 solution. Since the difference between the MRP1 and control vesicles was primarily the presence or absence of MRP1, these results suggest that only the MRP1 immobilized on the SLB interacted with the anti-MRP1. Another anti-MRP1 clone (MRPm5) having an epitope (amino acids 1063-1072) on the inside of cells *in vivo*[45] (Figure S5) was also evaluated (Figure 4b). Although the control vesicle-immobilizing surface showed nonspecific adsorption at higher concentrations (50 μg/mL), the Δλ value obtained with the MRP1 vesicle-immobilizing surface was larger than that observed with the control vesicle-immobilizing surface, just as was the case in the IU2H10 trials.

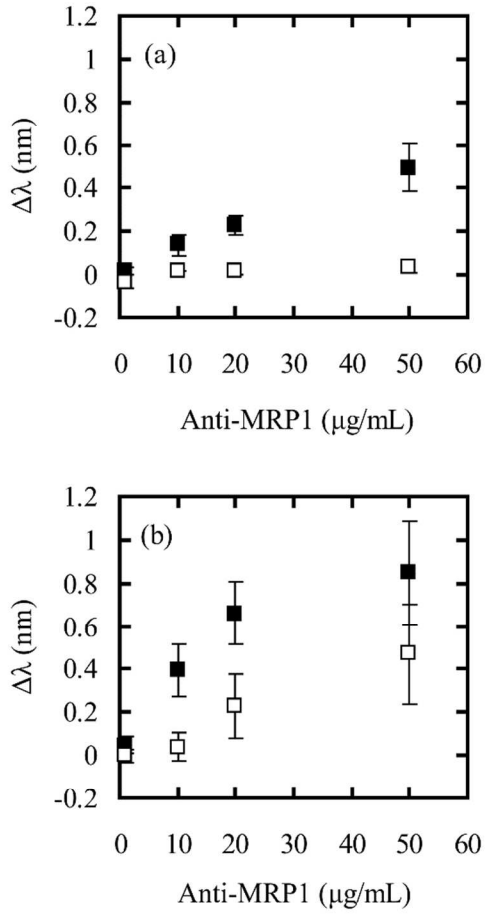

Figure 4. Reactivity of surface-immobilized vesicles with anti-MRP1: (a) clone: IU2H10 and (b) clone: MRPm5. Legend: solid square = MRP1, open square = control. Data points represent the mean ± one SD of triplicate determinations.

These results indicate that some moiety of the membrane protein that is recognized by MRPm5 was present on the sensing chip. When the membrane proteins are immobilized by vesicle fusion, the exteriors of the vesicles make contact with the substrate first, and therefore the majority of the vesicle interiors will be positioned upwards and thus able to interact with the antibodies. From the measurement results, anti-MRP1 molecules having their epitopes located both inside and outside cells can interact with MRP1 on an SLB prepared by vesicle fusion, since some MRP1 vesicles have been turned inside-out during the adsorption process.[46] In order to exclude the possibility of nonspecific protein-protein interactions between immunoglobulin and MRP1, anti-hIgG was applied to the RIfS sensor. Almost no response was observed to the anti-hIgG, confirming that the observed positive response to anti-MRP1 is caused by specific protein-protein interactions (Figure 5).

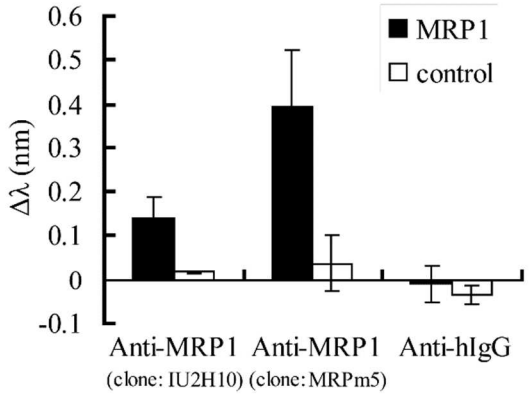

Figure 5. Selectivity of the vesicle-immobilizing surface for each antibody (10 μg/mL). Data points represent the mean ± one SD of triplicate determinations.

Conclusions

In conclusion, the present sensing system for membrane protein activity is advantageous because no special pre-treatment is required and the system is generated simply by injecting vesicles containing membrane proteins. Furthermore, the RIfS system has been shown capable of measuring changes in the film thickness, suggesting that conformational changes of the membrane proteins can be detected through interactions with small molecules, such as Trastuzumab (Genentech, San Francisco, CA, USA). Consequently, this work could provide a new means of detecting specific binding events on biological membranes, facilitating the development of assays based on membrane proteins for the detection of protein-protein (ligand) interactions and also therapeutic antibody discovery, quality control of antibody production and pre-screening prior to experiments on animals.

Acknowledgements

We thank Hideji Yokokura (KONICA MINOLTA, Inc., Tokyo, Japan) for TEM observations. We would also like to acknowledge Fuminori Okada and Manami Masubuchi, both of KONICA MINOLTA, for their contributions to this study. This work was supported in part by the Innovation Promotion Program of the New Energy and Industrial Technology Development Organization (NEDO), Kanagawa, Japan.

Notes and references

[a] Graduate School of Engineering, Kobe University, 1-1 Rokkodai-cho, Nada-ku, Kobe 657-8501, Japan; E-mail: takeuchi@gold.kobe-u.ac.jp

[b] KONICA MINOLTA, Inc., 1 Sakura-machi, Hino-shi, Tokyo 191-8511, Japan

† Electronic Supplementary Information (ESI) available: Characterization (contact angle measurements and ellipsometry) of ZrO_2 chips, physical thicknesses of immobilized vesicles, characterization data (dynamic light scattering and transmission electron microscopy) for vesicles, and topology of MRP1 are given in the supporting text and figures. See DOI: 10.1039/b000000x/

1 B. O. Yang, S. Xie, M. J. Berardi, X. Zhao, J. Dev, W. Yu, B. Sun and J. J. Chou, *Nature,* 2013, **498**, 521.

2 M. A. Hedinger, M. J. Coady, T. S. Ikeda and E. M. Wright, *Nature,* 2013, **330**, 379.

3 D. Torrents, R. Estévez, M. Pineda, E. Fernández, J. Lloberas, Y. B. Shi, A. Zorzano and M. Palacín, *J. Biol. Chem.,* 1998, **273**, 32437.

4 M. W. McEnery, A. M. Snowman, R. R. Trifiletti and S. H. Snyder, *Proc. Natl. Acad. Sci. USA,* 1992, **89**, 3170.

5 H. Wieczorek, *J. Exp. Biol.,* 1992, **172**, 335.

6 K. L. Pierce, R. T. Premont and R. J. Lefkowitz, *Nat. Rev. Mol. Cell Biol.,* 2002, **3**, 521.

7 A. A. Brian and H. M. McConnell, *Proc. Natl. Acad. Sci. USA,* 1984, **81**, 6159.

8 L. K. Tamm and H. M. McConnell, *Biophys. J.,* 1985, **47**, 105.

9 C. Larsson, M. Rodahl and F. Höök, *Anal. Chem.,* 2003, **75**, 5080.

10 R. P. Richter and A. R. Brisson, *Biophys. J.,* 2005, **88**, 3422.

11 K. Furukawa, K. Sumitomo, H. Nakashima, Y. Kashimura and K. Torimitsu, *Langmuir,* 2007, **23**, 367.

12 K. Tawa and K. Morigaki, *Biophys. J.,* 2005, **89**, 2750.

13 L. Gu, L. Wang, J. Xun and A. Ottova-Leitmannova, *Bioelectrochem. Bioenerg.,* 1996, **39**, 275.

14 J. T. Groves, N. Ulman and S. G. Boxer, *Science,* 1997, **275**, 651.

15 J. T. Groves and S. G. Boxer, *Acc. Chem. Res.,* 2002, **35**, 149.

16 T. Sandström, M. Stenberg and H. Nygren, *Appl. Opt.,* 1985, **24**, 472.

17 H. W. Choi, H. Takahashi, T. Ooya and T. Takeuchi, *Anal. Methods,* 2011, **3**, 1366.

18 H. W. Choi, Y. Sakata, Y. Kurihara, T. Ooya and T. Takeuchi, *Anal. Chim. Acta,* 2012, **728**, 64.

19 Y. Kurihara, M. Takama, T. Sekiya, Y. Yoshihara, T. Ooya and T. Takeuchi, *Langmuir,* 2012, **28**, 13609.

20 Y. Kurihara, M. Takama, M. Masubuchi, T. Ooya and T. Takeuchi, *Biosens. Bioelectron.,* 2013, **40**, 247.

21 H. W. Choi, Y. Sakata, T. Ooya, and T. Takeuchi, *J. Biosci. Bioeng.* 2014, in press. (DOI:10.1016/j.jbiosc.2014.06.017)

22 T. Fujimura, K. Takenaka and Y. Goto, *Jpn. J. Appl. Phys.,* 2005, **44**, 2849.

23 A. Murata, T. Ooya, and T. Takeuchi, *Microchim. Acta* 2014, in press. (DOI: 10.1007/s00604-014-1334-2)

24 P. K. Kanaujia, D. Pardasani, V. Tak, A. K. Purohit and D. K. Dubey, *J. Chromatogr. A,* 2011, **1218**, 6612.

25 H. Liu, X. Sun, C. Yin and C. Hu, *J. Hazard. Mater.,* 2008, **151**, 616.

26 B. P. Oberts and G. J. Blanchard, *Langmuir,* 2009, **25**, 2962.

27 R. M. Fabre and D. R. Talham, *Langmuir,* 2009, **25**, 12644.

28 R. M. Fabre, G. O. Okeyo and D. R. Talham, *Langmuir,* 2012, **28**, 2835.

29 S. P. C. Cole, G. Bhardwaj, J. H. Gerlach, J. E. Mackie, C. E. Grant, K. C. Almquist, A. J. Stewart, E. U. Kurz, A. M. Duncan and R. G. Deeley, *Science,* 1992, **258**, 1650.

30 R. G. Deeley, C. Westlake and S. P. C. Cole, *Physiol. Rev.,* 2006, **86**, 849.

31 D. R. Hipfner, R. G Deeley and S. P. C. Cole, *Biochim. Biophys. Acta,* 1999, **1461**, 359.

32 G. M. Hale and M. R. Querry, *Appl. Opt.,* 1973, **12**, 555.

33 M. Gagoś, R. Koper and W. I. Gruszecki, *Biochim. Biophys. Acta,* 2001, **1511**, 90.

34 A. Sujak, J. Gabrielska, J. Milanowska, P. Mazurek, K. Strzałka and W. I. Gruszecki, *Biochim. Biophys. Acta,* 2005, **1712**, 17.

35 J. F. Masson, L. Obando, S. Beaudoin and K. Booksh, *Talanta,* 2004, **62**, 865.

36 P. Luckham, J. Wood, S. Froggatt and R. Swart, *J. Colloid Interface Sci.,* 1992, **153**, 368.

37 M. Takizawa, Y. H. Kim and T. Urisu, *Chem. Phys. Lett.,* 2004, **385**, 220.

38 S. B. Lei, R. Tero, N. Misawa, S. Yamamura, L. J. Wan and T. Urisu, *Chem. Phys. Lett.,* 2006, **429**, 244.

39 P. S. Cremer and S. G. Boxer, *J. Phys. Chem. B,* 1999, **103**, 2554.

40 S. A. Simon and T. J. McIntosh, *Biochim. Biophys. Acta,* 1984, **773**, 169.

41 J. F. Nagle and M. C. Wiener, *Biochim. Biophys. Acta,* 1988, **942**, 1.

42 R. M. Fabre and D. R. Talham, *Langmuir,* 2009, **25**, 12644.

43 U. Seifert and R. Lipowsky, *Phys. Rev. A,* 1990, **42**, 4768.

44 Q. Chen, Y. Yang, Y. Liu, B. Han and J. T. Zhang, *Biochemistry,* 2002, **41**, 9052.

45 K. Koike, R. G. Deeley and S. P. C. Cole, *Biochim. Biophys. Res. Commun.,* 2004, **315**, 719.

46 V. L. Lew, A. Hockaday, C. J. Freeman and R. M. Bookchin, *J. Cell Biol.,* 1988, **106**, 1893.